Anion-Sensitive Fluorophore Identifies the Drosophila Swell-Activated Chloride Channel in a Genome-Wide RNA Interference Screen

OPEN ACCESS Freely available online

PLOS ONE

Anion-Sensitive Fluorophore Identifies the *Drosophila* Swell-Activated Chloride Channel in a Genome-Wide RNA Interference Screen

Stephanie C. Stotz[1], David E. Clapham[1,2,3]*

1 Howard Hughes Medical Institute, Department of Cardiology, Boston Children's Hospital, Boston, Massachusetts, United States of America, **2** Manton Center for Orphan Disease, Boston Children's Hospital, Boston, Massachusetts, United States of America, **3** Department of Neurobiology, Harvard Medical School, Boston, Massachusetts, United States of America

Abstract

When cells swell in hypo-osmotic solutions, chloride-selective ion channels (Cl_{swell}) activate to reduce intracellular osmolality and prevent catastrophic cell rupture. Despite intensive efforts to assign a molecular identity to the mammalian Cl_{swell} channel, it remains unknown. In an unbiased genome-wide RNA interference (RNAi) screen of *Drosophila* cells stably expressing an anion-sensitive fluorescent indicator, we identify Bestrophin 1 (dBest1) as the *Drosophila* Cl_{swell} channel. Of the 23 screen hits with mammalian homologs and predicted transmembrane domains, only RNAi specifically targeting dBest1 eliminated the Cl_{swell} current ($I_{Clswell}$). We further demonstrate the essential contribution of dBest1 to *Drosophila* $I_{Clswell}$ with the introduction of a human Bestrophin disease-associated mutation (W94C). Overexpression of the W94C construct in *Drosophila* cells significantly reduced the endogenous $I_{Clswell}$. We confirm that exogenous expression of dBest1 alone in human embryonic kidney (HEK293) cells creates a clearly identifiable *Drosophila*–like $I_{Clswell}$. In contrast, activation of mouse Bestrophin 2 (mBest2), the closest mammalian ortholog of dBest1, is swell-insensitive. The first 64 residues of dBest1 conferred swell activation to mBest2. The chimera, however, maintains mBest2-like pore properties, strongly indicating that the Bestrophin protein forms the Cl_{swell} channel itself rather than functioning as an essential auxiliary subunit. dBest1 is an anion channel clearly responsive to swell; this activation depends upon its N-terminus.

Citation: Stotz SC, Clapham DE (2012) Anion-Sensitive Fluorophore Identifies the *Drosophila* Swell-Activated Chloride Channel in a Genome-Wide RNA Interference Screen. PLoS ONE 7(10): e46865. doi:10.1371/journal.pone.0046865

Editor: Alexander A. Mongin, Albany Medical College, United States of America

Received June 12, 2012; **Accepted** September 6, 2012; **Published** October 4, 2012

Funding: SCS is supported by the Tommy Kaplan Fellowship, Boston Children's Hospital, Boston. Howard Hughes Medical Institute provided funding for this study. The funders had no role in study design, data collection and analysis, decision to publish, or preparation of the manuscript.

Competing Interests: The authors have declared that no competing interests exist.

* E-mail: dclapham@enders.tch.harvard.edu

Introduction

All mammalian cells express chloride channels activated by decreases in extracellular osmolality, albeit with different biophysical properties [1]. The ubiquitous expression of Cl_{swell} suggests its essential cellular function. Tightly regulated Cl_{swell} channels participate in volume regulation, motility, cell survival, and cell division [1]. In contrast, de-regulated constitutively active Cl_{swell} channels exacerbate several cardiac diseases, including myocardial hypertrophy and heart failure [2]. The mammalian Cl_{swell} channel- encoding gene has yet to be identified despite the wealth of proteins nominated by candidate approaches [3]. These proteins include ClC-2 [4], ClC-3 [5], P-glycoprotein [6,7], pICln [8,9], p64 [10], phospholemman [11], Best1 and 2 [12], TMEM16A [13], and TMEM16F [14]. The research community has yet to agree on any of these candidates as a *bona fide* Cl_{swell} channel.

In *Drosophila*, however, accumulating evidence indicates that *dBest1* encodes for a Cl_{swell} channel. RNAi targeting *dBest1* eliminates *Drosophila* Schneider (S2) cell $I_{Clswell}$, an effect rescued by re-introduction of dBest1 [15]. Further, swell activated dBest1 mutants have altered biophysical properties and reactivity to sulfhydryl reagents [16]. dBest1 likely forms the chloride conducting pore, but it may be an obligate auxillary subunit of *Drosophila* $I_{Clswell}$ that modifies channel properties akin to CaV β subunits [17].

Assigning chloride channel function to any protein is difficult. The known chloride channel families (*e.g.*, ClC, Anoctamin/TMEM16, CFTR, and ionotropic $GABA_A$ and GlyR) lack structural pore or gating motifs that might form the basis for *in silico* identification. Expression cloning approaches have also failed due to widespread Cl_{swell} channel expression that precludes the separation of endogenous and over-expressed protein activities. Moreover, known chloride channels blockers are non-specific and their affinities are far too low to encourage affinity purification. Finally, previous chloride indicators are poor tools for screening due to loading and retention issues, inconsistent results, and poor reproducibility [18].

Here we present an unbiased genome-wide, high-throughput RNAi screen designed to identify the *Drosophila* Cl_{swell} channel and its regulators. Our screen employed H148Q-YFP, a genetically encoded anion-sensitive yellow fluorescent protein [19], to report Cl_{swell} activity in *Drosophila* S2R+ cells. Of our 595 initial hits that altered chloride handling, we concentrated on characterizing proteins with mammalian homology and at least one transmembrane domain as potential Cl_{swell} channels. dBest1 emerged from our screen as the lead candidate for *Drosophila* Cl_{swell}. Both RNAi

knockdown of dBest1 and overexpression of a dominant-negative dBest1 eliminated the Cl_{swell} current in *Drosophila* S2R+ cells. Conversely, dBest1 overexpression in a mammalian system (HEK cells) produced a *Drosophila*–like $I_{Clswell}$. To identify domains necessary for swell activation we characterized chimeras between the swell-sensitive dBest1 and the swell-insensitive mBest2. Swell sensitivity is only apparent in mBest2, the closest mammalian homolog of dBest1, when the protein contains the dBest1 amino (N)-terminus. This chimera maintains the pore properties of mBest2, providing additional evidence that the protein itself forms a channel rather than functioning as a necessary auxiliary subunit. We conclude that dBest1 is the channel underlying the *Drosophila* $I_{Clswell}$.

Results

Drosophila S2R+ Cells have Robust $I_{Clswell}$

Drosophila S2 cells are used extensively in genome-wide RNAi screens to dissect signaling pathways, determine protein functions, and assign protein molecular identity [20]. These macrophage-like cells, derived from primary culture of late stage *Drosophila melanogaster* embryos [21] readily take up RNAi from serum-free media. The subsequent process of targeted mRNA ablation is efficient and highly reproducible [22,23]. For our screen we used S2R+ cells [24], an adherent S2 variant well suited for assays that require multiple solution changes. Importantly, S2R+ cells have a consistent, large $I_{Clswell}$ that activates slowly upon a drop in extracellular osmolality (Figure 1A). $I_{Clswell}$ starts to activate within 2 min exposure to hypo-osmotic media, reaching steady state activation by 5 min. The fully activated Cl_{swell} conductance is anion selective (Figure 1B). The relative permeability sequence of S2R+ Cl_{swell} is I = SCN>Cl>MES>aspartate (ASP) while the slope conductance sequence is I = SCN = Cl>MES>ASP (Table 1 & 2). The Cl_{swell} I–V relationship has a slight "S" shape, revealing rectification. An extended step protocol further illustrates features of S2R+ Cl_{swell} (Figure 1C). $I_{Clswell}$ exhibits an initial instantaneous activation followed by a second slow activation phase, suggesting that more than one type of Cl^- conductance is turned on in S2R+ cells with cell swelling. In contrast, Chien & Hartzell [15] reported a single phase, time-independent $I_{Clswell}$ activation in their S2 cells, perhaps indicating Cl^- channel expression differences in the two cell lines. Tail currents, normally indicating time dependence of deactivation of the channel, are evident in our recordings. However, since tail currents were not observed under symmetrical recording conditions [15], we attribute these currents to the exit of intracellular Cl^- accumulated during the prolonged steps. S2R+ $I_{Clswell}$ has an interesting pharmacological profile (Figure 2A). Even at a high concentration (100 μM), the non-specific chloride channel blocker 4,4′-diisothiocyano-2,2′-stilbenedisulfonic acid (DIDS) [25] blocks less than 25% of the S2R+ $I_{Clswell}$ (Figure 2A). 4-2(2-butyl-6,7-dichloro-2-cyclopentyl-indan-1-on-5-yl (DCPIB), a mammalian selective $I_{Clswell}$ blocker [26], fails to completely block S2R+ $I_{Clswell}$ at 30 μM (Figure 2A & E). DCPIB blocks in a voltage-dependent manner (Figure 2E); at 0 mV 52**%** of S2R+ $I_{Clswell}$ is blocked, while 90**%** is blocked at 80 mV. Surprisingly, furosemide, a Na-K-2Cl cotransporter (NKCC; SLC12A2) blocker, almost completely inhibits S2R+ $I_{Clswell}$ at 1 mM (Figure 2A & 3C).

H148Q-YFP Reliably Reports the Activity of S2R+ Cell Cl_{swell} Channels

Cl_{swell} conducts iodide better than chloride, favoring the use of the H148Q-YFP indicator as a reporter of its activity (I^- K_D = 20 mM and Cl^- K_D = 100 mM [19,27,28]). Several anion-sensitive YFP variants accurately quantify intracellular Cl^- concentration or changes [27,29–31]; anion binding near the YFP chromophore suppresses fluorescence emission by altering chromophore resonance [19]. H148Q-YFP was chosen for Cl_{swell} detection because it is bright and potently suppressed by I^-; these properties are critical for good signal-to-noise ratios during screening. H148Q-YFP (pK_a = 6.7) is also sensitive to intracellular pH changes [19,28]. S2R+ cells stably expressing H148Q-YFP maintain their fluorescence in 240 mOSM NaCl however (Figure 3A), indicating that cell swelling does not appreciably alter intracellular pH. Subsequent replacement of bath Cl^- with I^- rapidly suppresses indicator fluorescence by 50% as I^- enters the cells through open channels and interacts with the probe. The large fluorescence change and low intrinsic assay variability favor clear separation of potential hits. In the absence of hypo-osmotic solution, I^- is unable to enter the S2R+ cells and fluorescence is maintained (Figure 3B), indicating that S2R+ cells lack alternative constitutively active I^- entry pathways that could confound our ability to identify the Cl_{swell} channel. Further, furosemide block of open Cl_{swell} channels prevents appreciable fluorescence suppression (Figure 3C & D), suggesting that RNAi effectively targeting the Cl_{swell} channel will be readily identifiable as hits.

Genome-wide RNAi Screening of H148Q-YFP S2R+ Cells Identifies dBest1 as the Cl_{swell} Channel

The primary screen was conducted at the Harvard/HHMI *Drosophila* RNAi Screening Center using our stable H148Q-YFP-expressing S2R+ cell line. Each well of sixty-six 384-well assay plates contained a dsRNA targeting 1 of 13,900 genes encoding proteins or non-coding RNAs (DRSC 2.0; Figure 4A). Five days after S2R+ cells were treated with RNAi, we assessed cellular fluorescence under swell conditions in the presence of Cl^- and I^-. Wells with fluorescence or ratio (I^- fluorescence/Cl^- fluorescence) changes greater than 1.5 times the standard deviation of the plate mean were initially considered as hits (Cl_{swell} channel candidates or regulators of its activation pathway). We pared the list of 595 hits to genes with mammalian homologs and those with predicted transmembrane domains (Figure 4B, *Table S1*). In a secondary screen, we confirmed that each RNAi significantly reduced swelling-induced fluorescence and targeted only the mRNA from the identified gene (qPCR). We then directly measured $I_{Clswell}$ via whole-cell voltage clamp. Candidates genes, whose RNAi significantly reduced the S2R+ cell $I_{Clswell}$, were cloned and expressed in HEK293 or CHO-K1 cells. $I_{Clswell}$ was then measured via whole-cell recording and compared with currents from untransfected cells. The only candidate of our screen to satisfy all the criteria for a Cl_{swell} channel was dBest1 (*Table S1*).

DRSC26457 RNAi Targeting dBest1 Eliminates $I_{Clswell}$

dBest1 is a protein of 769 amino acids containing 4 transmembrane domains [32,33] (Figure 4C). It is one of four Bestrophin family members in *Drosophila*, with highest homology to mBest2/hBest2 (51% identity and 67% similarity; BLAST). Hartzell and colleagues first proposed that dBest1 was a chloride channel activated by high intracellular Ca^{2+} and cell swelling [15,16]. In our H148Q-YFP fluorescence assay dBest1 RNAi DRSC26457 abrogated the fluorescence change normally observed when I^- enters the S2R+ cells through activated Cl_{swell} conductances (Figure 5A, B). Interestingly, DRSC26457 also decreased the baseline fluorescence variability of S2R+ cells (Figure 5B), suggesting that I_{dBest1} contributes to resting intracellular Cl^- concentrations. S2R+ $I_{Clswell}$ was essentially eliminated by dBest1 RNAi DRSC26457 treatment (Figure 5C). This RNAi specifically and effectively reduced dBest1 mRNA by 91.5% ±0.5

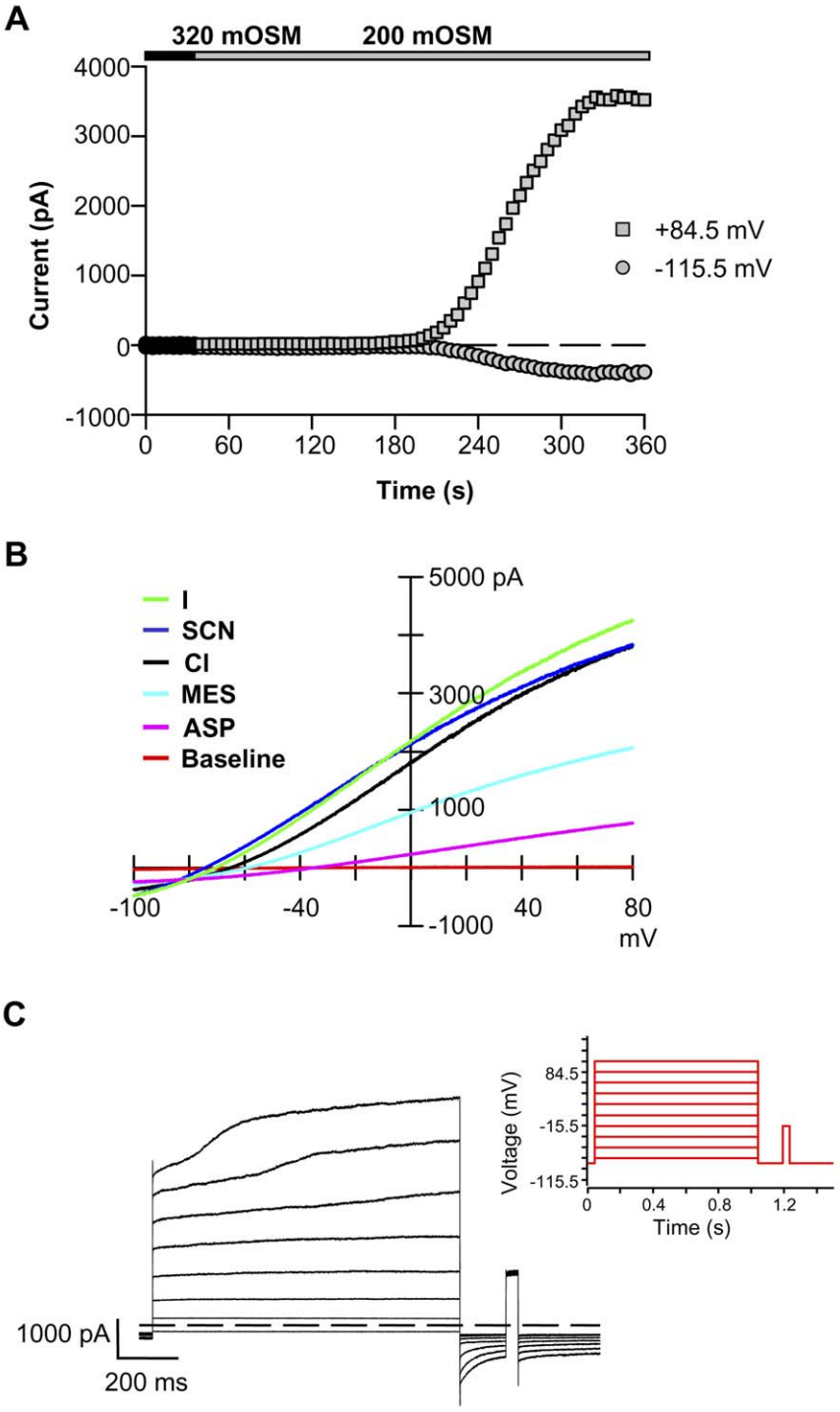

Figure 1. Characterization of the S2R+ cell $I_{Clswell}$. (**A**) Hypo-osmotic solutions slowly activate $I_{Clswell}$. $I_{Clswell}$ begins to activate 1.7±0.3 min after exposure to 200 mOSM solution and reaches steady state activation within 5±0.3 min (n = 13). $I_{Clswell}$ was assessed in ramp protocols and reported at +84.5 mV (upper trace) and -115.5 mV (lower trace). 240 mOSM stimulates $I_{Clswell}$ activation slightly more slowly (1.8±0.3 min to initiation and 5.2±0.6 min to steady state, n = 12; data not shown). (**B**) The S2R+ cell $I_{Clswell}$ is anion-selective. $I_{Clswell}$ was activated by 200 mOSM solution; relative permeability and slope conductance sequences were determined for the steady state $I_{Clswell}$ by replacing Cl^- with equimolar anion concentrations. (**C**) An extended step protocol (red inset) reveals more than one set of activation kinetics with offset activation initiation times.
doi:10.1371/journal.pone.0046865.g001

(n = 3; qPCR); mRNA levels for the 3 remaining Bestrophin members and other Cl_{swell} candidates were unaffected. A second RNAi targeting dBest1 (DRSC16909; corresponds with dB1S [15]) was part of our initial screen. It was less effective at knocking down dBest1 mRNA (85% reduction, n = 3; significantly less than DRSC26457; $p<0.001$, Student's t-test) and had two predicted off-target hits: CG4623 (20/20) and CG16711 (18/18). DRSC16909 did not significantly alter H148Q-YFP I^- induced

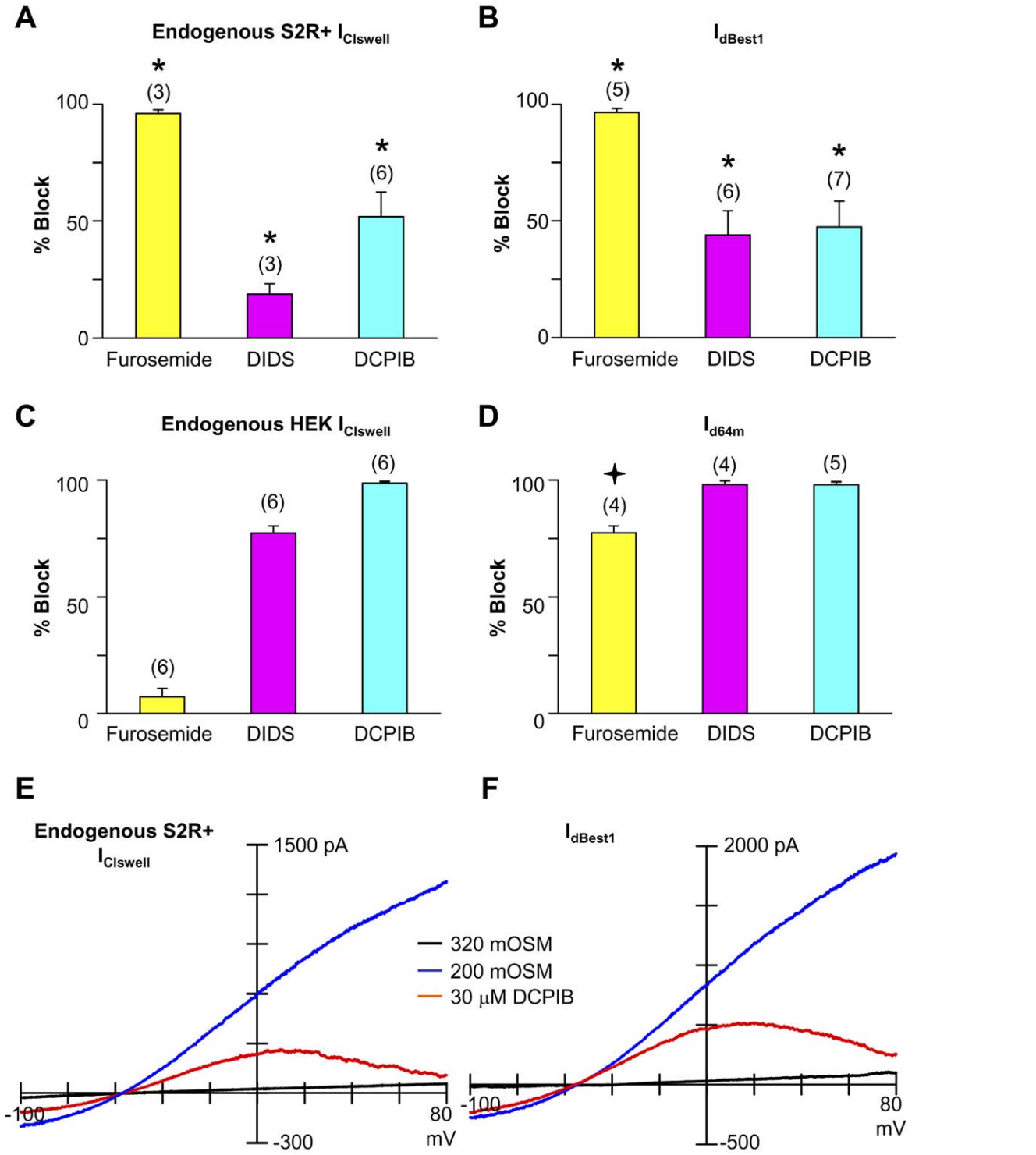

Figure 2. Pharmacological profiles of S2R+ $I_{Clswell}$ and I_{dBest1} match and differ from those of HEK $I_{Clswell}$ and I_{d64m}. (A–D) % Block of S2R+ $I_{Clswell}$, I_{dBest1}, HEK $I_{Clswell}$ and I_{d64m} by 1 mM furosemide, 100 μM DIDS, and 30 μM DCPIB. Block at 0 mV is presented to emphasize the incomplete voltage-dependent DCPIB block of S2R+ $I_{Clswell}$ and I_{dBest1}. (A) Steady state S2R+ $I_{Clswell}$ activated by 200 mOSM stimulation was blocked 96% ±1.6 by furosemide, 19% ±4 by DIDS, and 52% ±10.6 by DCPIB. * no difference compared to I_{dBest1} block and significantly different compared to HEK $I_{Clswell}$ and I_{d64m} (ANOVA, $p<0.05$). (B) I_{dBest1}, stimulated for 2 min by 200 mOSM, was blocked 96% ±1.7 by furosemide, 44% ±10 by DIDS, and 47% ±10.9 by DCPIB. * no difference compared to S2R+ $I_{Clswell}$ block and significantly different compared to HEK $I_{Clswell}$ and I_{d64m} (ANOVA, $p<0.05$). (C) Steady-state HEK $I_{Clswell}$ activated by 200 mOSM stimulation was blocked 7% ±3.5 by furosemide, 77% ±3 by DIDS, and 99% ±0.7 by DCPIB. (D) Constitutive I_{d64m} (320 mOSM) was blocked 77% ±3 by furosemide, 98% ±1.5 by DIDS, and 98% ±1.2 by DCPIB. ✦ significantly different compared to S2R+ $I_{Clswell}$, HEK $I_{Clswell}$ and I_{d64m} (ANOVA, $p<0.05$). (E–F) I–V relations for S2R+ $I_{Clswell}$ and I_{dBest1} demonstrate DCPIB voltage-dependent block. At 80 mV, DCPIB block of S2R+ $I_{Clswell}$ is 90% ±3.6 ($n=6$), and 82% ±6.5 for I_{dBest1} ($n=7$).
doi:10.1371/journal.pone.0046865.g002

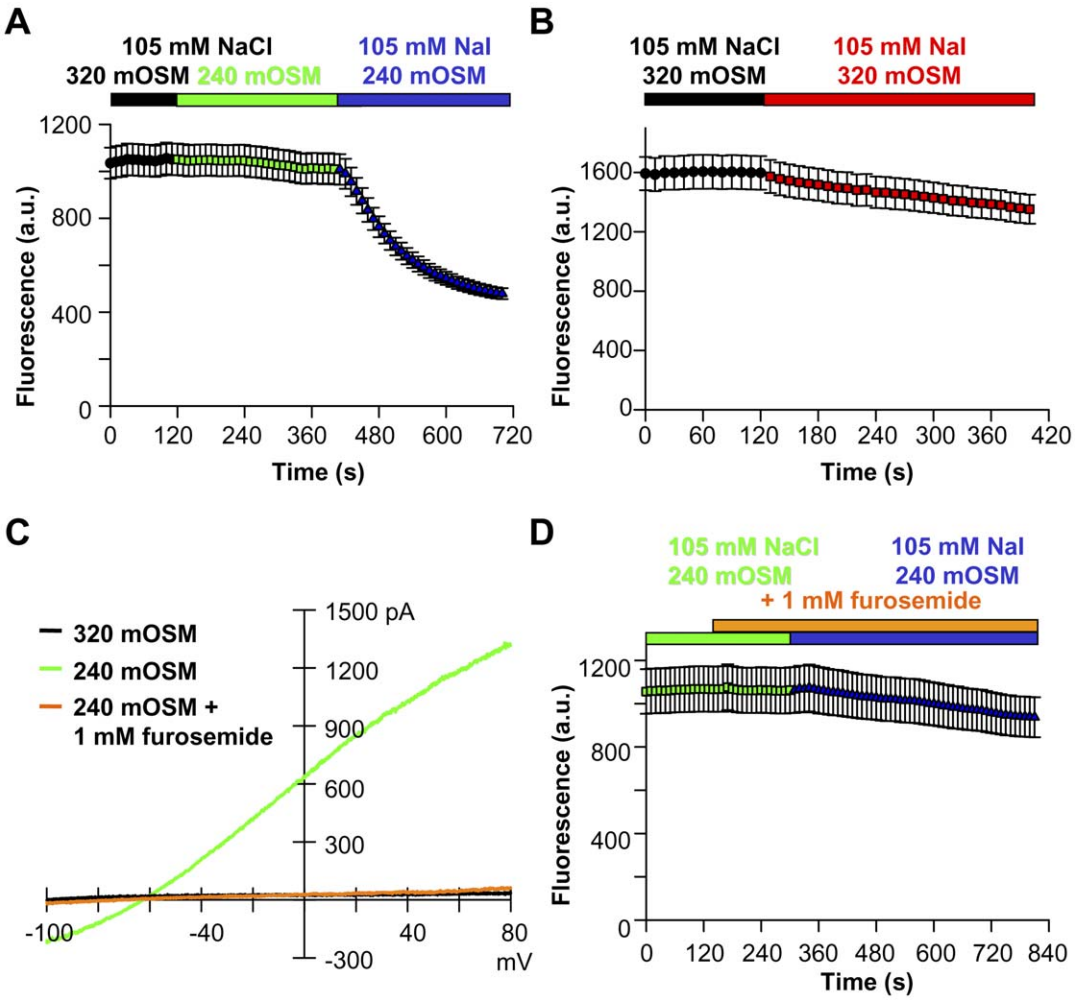

Figure 3. H148Q-YFP stably expressed in S2R+ cells reports the entry of I^- through activated Cl_{swell} channels. (**A**) Cellular swelling in 240 mOSM Cl^- did not alter fluorescence intensity as Cl_{swell} channels activate (Student's t-test, $p = 0.65$; $n = 76$). Replacement of Cl^- with I^- evoked a 51% ±1.3 decrease in fluorescence (Student's t-test, $p < 0.001$; $n = 76$). Imaging assay; fluorescence is in arbitrary units (a.u.). (**B**) Cl_{swell} channels must be open for I^-induced fluorescence suppression to occur. 320 mOSM NaI suppresses fluorescence by 16% ±0.7 (Student's t-test, $p = 0.1$; $n = 54$). (**C**) Furosemide, an NKCC2 blocker, completely inhibits the S2R+ cell Cl_{swell} channels at 1 mM ($n = 3$). (**D**) 1 mM Furosemide block of Cl_{swell} prevents significant I^-induced suppression of H148Q-YFP fluorescence (Student's t-test, $p = 0.54$; $n = 16$).
doi:10.1371/journal.pone.0046865.g003

fluorescence suppression (Figure 5A), and was not a hit in our initial screen. It is possible that the 15% remaining mRNA translated sufficient amounts of functional dBest1/Cl_{swell} channels to exclude it as a hit in our screen. This prospect emphasizes the importance of validated, effective RNAi for accurate screening.

Mutant dBest1 W94C Significantly Reduces S2R+ $I_{Clswell}$

To substantiate the conclusion that dBest1 is an essential component of the Cl_{swell} channel, we tested whether a mutant dBest1 would act as a dominant negative regulator of $I_{Clswell}$. In humans, Bestrophin 1 is mutant in vitelliform macular dystrophy

Table 1. Relative Permeabilities.

	P_X/P_{Cl}					n
	I	SCN	Cl	MES	ASP	
S2R+	1.5±0.12	1.6±0.15	1	0.74±0.15	0.07±0.015	3
dBest1	1.8±0.05	2±0.04	1	0.63±0.04	0.09±0.0017	5
mBest2	1.7±0.15	2.9±0.68	1	0.45±0.14	0.05±0.006	6
d64m	2.2±0.34	2.6±0.11	1	0.43±0.14	0.07±0.011	4
HEK	1.5±0.06	1.8±0.2	1	0.62±0.005	0.11±0.003	6

doi:10.1371/journal.pone.0046865.t001

Table 2. Slope Conductance.

	Slope Conductance (G; I/V)					n
	I	SCN	Cl	MES	ASP	
S2R+	29.6±6.8	26.9±5.9	28±7.5	16.4±3.5	7.6±1.5	3
dBest1	8.2±1.5	6.6±1.1	5.2±0.7	3.3±0.4	1.9±0.3	5
mBest2	10±4.9	2.4±0.95	6.6±3.4	2±1.3	1.7±1.1	6
d64m	10±3.5	2.5±0.36	4.4±0.3	1.9±0.5	1.7±0.3	3
HEK	26.2±8.2	24.9±7.1	26.9±7.9	9.5±5.4	5.4±2.7	6

doi:10.1371/journal.pone.0046865.t002

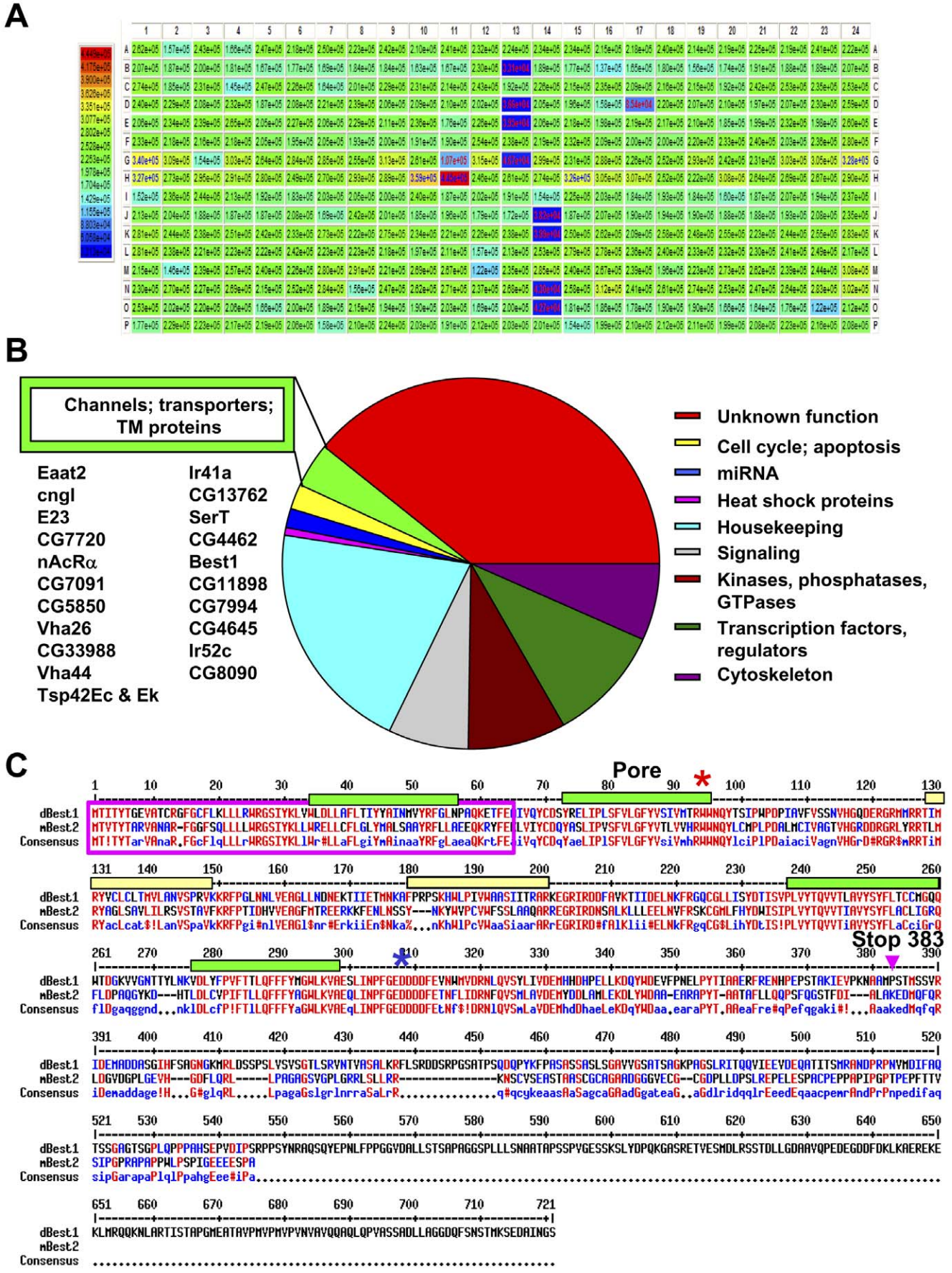
A
B
Channels; transporters; TM proteins
Eaat2
cngl
E23
CG7720
nAcRα
CG7091
CG5850
Vha26
CG33988
Vha44
Tsp42Ec & Ek
Ir41a
CG13762
SerT
CG4462
Best1
CG11898
CG7994
CG4645
Ir52c
CG8090
Unknown function
Cell cycle; apoptosis
miRNA
Heat shock proteins
Housekeeping
Signaling
Kinases, phosphatases, GTPases
Transcription factors, regulators
Cytoskeleton
C
Pore
Stop 383
dBest1
mBest2
Consensus

Figure 4. Genome-wide RNAi screening of H148Q-YFP S2R+ cells identifies Cl_{swell} channel candidates and regulators. (**A**) RNAi treatment alters S2R+ cell H148Q-YFP fluorescence levels. Heat map plate reader data following 5d RNAi treatment (240 mOSM Cl^-). Fluorescence was subsequently measured in 240 I^-. Wells where the I^- to Cl^-fluorescence ratio was high are hits. Control RNAis are found in columns 13 and 14. Thread RNAi is in 13B, 13G, 14K, and 14N. Rho RNAi is in 13D, 13E, 14J, and 14O. GFP RNAi is in 13C, 13F, 14L, and 14M. Wells with elevated fluorescence in 240 mOSM Cl^- are shown in red and orange. (**B**) Functional classification of the 595 hits identified in our screen. 21 hits were transmembrane proteins of unknown function, putative ion channels, or transporters. 9 candidates with human homology were further evaluated (Table S1). (**C**) Protein sequence alignment of dBest1 and mBest2 (Multalign; multalin.toulouse.inra.fr/multalin/). Green bars indicate transmembrane domains. Yellow bars indicate other putative α-helices (SOSUI; bp.nuap.nagoya-u.ac.jp/sosui/). A red star indicates the W94C mutation. A blue star indicates the Ca^{2+}-binding bowl. A pink arrow indicates Stop 383. A pink box outlines the region switched in the d64m chimera.
doi:10.1371/journal.pone.0046865.g004

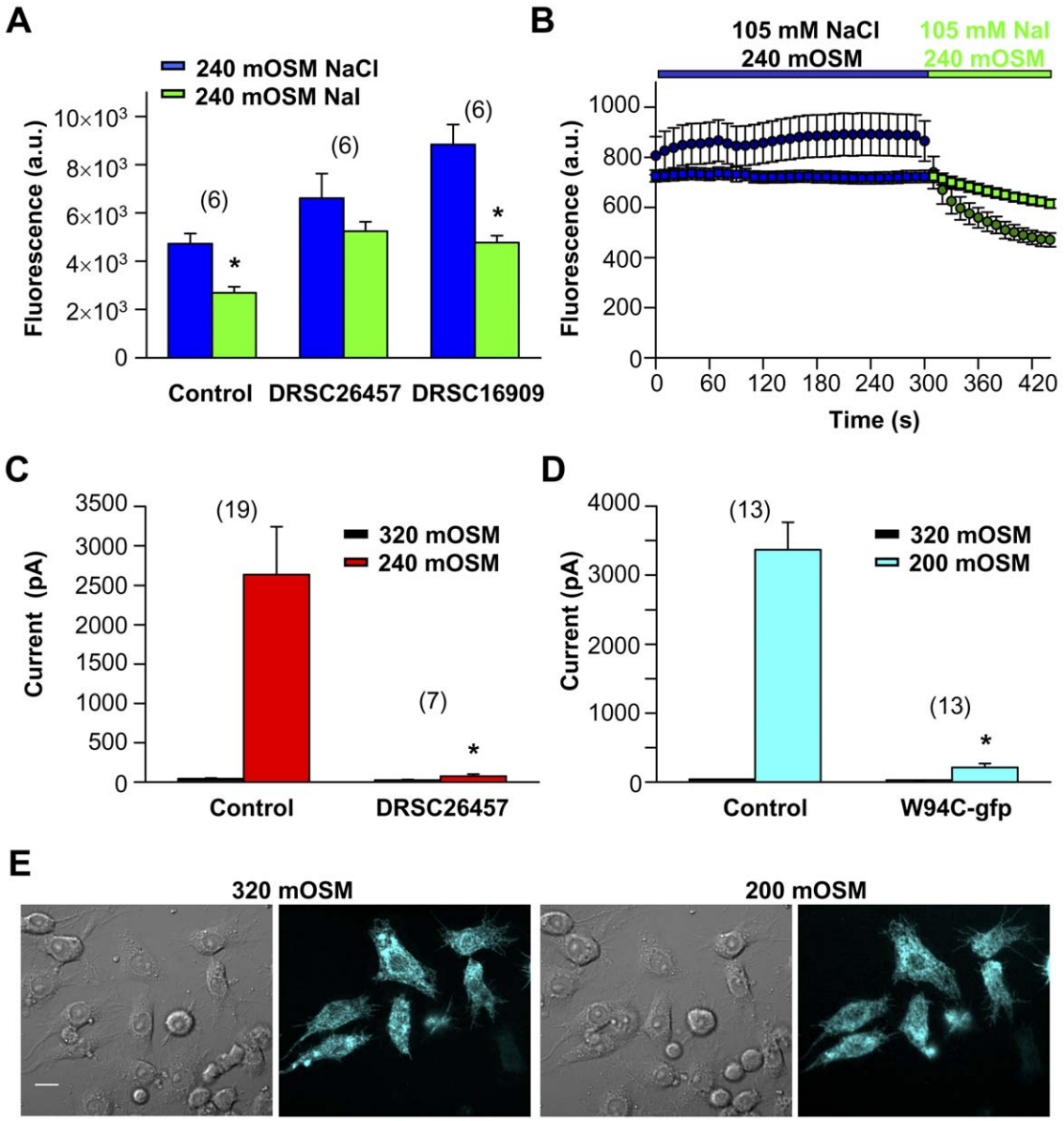

Figure 5. DRSC26457 identifies dBest1 as Cl_{swell}. (**A & B**) RNAi efficiently targeting dBest1 prevents significant I^-induced H148Q-YFP suppression following hypo-osmotic stimulation. Fluorescence is in arbitrary units (a.u.). (**A**) Plate reader assay. DRSC26457 RNAi treatment resulted in a fluorescence decrease of 6.4% ±19. Control and DRSC16909 RNAi treatment resulted in fluorescence decreases of 40.5% ±9.1 and 43.7% ±6.2 respectively. * 240 mOSM NaCl and NaI fluorescence levels are significantly different (Student's t-test, $p<0.05$). (**B**) Imaging assay. The fluorescence levels of individual S2R+ cells treated with control or dBest1 DRSC26457 RNAi were measured during hypo-osmotic stimulation in the sequential presence of Cl^- and I^-. The fluorescence of control cells decreased by 56% (n = 44); in contrast, the fluorescence of dBest1 DRSC26457 RNAi treated cells was suppressed by 15% (n = 174). (**C**) dBest1 DRSC26457 RNAi eliminated $I_{Clswell}$ in S2R+ cells. Following dBest1 RNAi treatment I_{320} is not significantly different from I_{240} (Student's t-test, p = 0.1). * control and RNAi treated I_{240} are significantly different (Student's t-test, p = 0.02). (**D**) dBest1 W94C-gfp overexpression suppresses S2R+ $I_{Clswell}$. * control and W94C-gfp $I_{200\ mOSM}$ are significantly different (Student's t-test, p = 0.02). (**E**) Confocal images of dBest1 W94C-gfp overexpression in S2R+ cells. Images were obtained before (320 mOSM) and after swell (200 mOSM). Scale bar indicates 10 μm.
doi:10.1371/journal.pone.0046865.g005

(Best's disease [34,35]). One mutation, W93C, occurs in a conserved sequence of the channel's putative pore [36,37] (Figure 4C). When we expressed the homolog dBest1 W94C-gfp in S2R+ cells, $I_{Clswell}$ was significantly reduced (Figure 5D). Interestingly, the late activating component of $I_{Clswell}$ remained clearly evident at depolarized potentials (Figure S1). We could not study this current in more detail as a loss of cell membrane integrity rapidly ensued. We conclude that dBest1 is responsible for the early activating S2R+ cell $I_{Clswell}$. W94C might interact with WT dBest1 to disrupt the Cl_{swell} channel pore or it may prevent proper protein trafficking [38]. In S2R+ cells, dBest1 W94C-gfp has a distinct intracellular expression pattern unaltered by osmotic changes (Figure 5E), suggesting the latter explanation over the former. Regardless, dBest1 W94C has a dominant negative impact on $I_{Clswell}$, further evidence that dBest1 is integral to the Cl_{swell} channel.

Another disease-associated Bestrophin mutation, D308A, occurs in a putative Ca^{2+} -binding bowl located in the channel's C-terminus (Figure 4C; blue star). D308A is proposed to eliminate Bestrophin activation by disruption of calcium binding [39]. We introduced this mutation into dBest1 to determine if activation by calcium and cell swelling could be separated. Unfortunately dBest1 D308A-gfp was not functional in HEK cells (data not shown). Three possible explanations may underlie this result: 1) activation by multi-modal stimuli is simultaneously disrupted by the mutation; 2) the mutation causes protein misfolding and the channel function has been eliminated for reasons unrelated to activation; 3) the mutant channel is mislocalized. Our GFP-tagged protein was expressed (data not shown), but we cannot exclude the possibility that it mislocalizes or fails to interact appropriately with other proteins necessary for $I_{Clswell}$ activation or channel function [34].

Exogenous dBest1 Expression Creates a *Drosophila*-like $I_{Clswell}$

Exogenous expression of a candidate protein substantiates whether the protein is necessary and/or sufficient in a given process. Our secondary screen assessed whether candidate protein expression resulted in a novel $I_{Clswell}$ or augmented the endogenous HEK $I_{Clswell}$ (*Table S1*). The HEK cell line chosen for candidate over-expression lacked constitutive I_{Cl} and I_{SCN} (potentially contaminating conductances attributable to SLC1A family member expression [40]; data not shown). The endogenous HEK $I_{Clswell}$ develops very slowly (Figure 6A & B); a two fold increase was noted within the first 2 min of swell. Once the HEK $I_{Clswell}$ reaches steady state, however, it has increased more than forty fold (44.4 ± 10.7 fold, $n = 29$; Student's t-test, $p < 0.000005$). Tail currents are absent (Figure 6B & C). Characteristic voltage-dependent inactivation develops during steps to positive potentials (Figure 6C). HEK $I_{Clswell}$ is anion selective; its permeability and conductance sequences match closely to those of S2R+ $I_{Clswell}$ (Figure 6D; Table 1 & 2). The HEK $I_{Clswell}$ pharmacological profile (Figure 2C) correlates well with the literature. 100 μM DIDS, slightly above the reported IC_{50} [41], blocks 78% of the HEK $I_{Clswell}$ at +80 mV (Figure 2C). DCPIB has an IC_{50} of 4 μM [26]; at 30 μM 100% of HEK $I_{Clswell}$ is blocked (Figure 2C). 1 mM furosemide barely inhibits HEK $I_{Clswell}$ (Figure 2C). The endogenous HEK $I_{Clswell}$ recapitulates the key features noted for the mammalian $I_{Clswell}$ [1].

Bestrophin proteins are not universally accepted as *bona fide* chloride channels; alternatively they are intracellular ion channel regulators [33,42,43]. dBest1-gfp is clearly observed on or near the surface of HEK-293 cells (Figure 7A). Its expression results in a *Drosophila*-like $I_{Clswell}$ (Figure 7B–E). Constitutively active I_{dBest1} is apparent in iso-osmotic 320 mOSM solution and is significantly increased 16 ± 4.5 fold (Student's t-test, $p < 0.005$) during the first 2 min of hypo-osmotic stimulation (Figure 7B). I_{dBest1} has the same "S"-shaped rectification as *Drosophila* $I_{Clswell}$ during ramps (Figure 7C); tail currents and time-dependent activation are both apparent in the step protocol (Figure 7d). I_{dBest1} is anion selective; it has the same permeability and conductance sequences as S2R+ $I_{Clswell}$ and HEK $I_{Clswell}$ (Figure 7E; Table 1 & 2). Strikingly, I_{dBest1} and the endogenous S2R+ $I_{Clswell}$ share a similar pharmacological profile that differs significantly from HEK $I_{Clswell}$ (Figure 2A–C). 100 μM DIDS inhibits 35% of I_{dBest}, while 30 μM DCPIB blocks 45%. 1 mM furosemide blocks nearly 100% of the I_{dBest1}. We conclude that dBest1 expression results in a *Drosophila*-like $I_{Clswell}$; it cannot be attributed to endogenous HEK $I_{Clswell}$ upregulation.

dBest1 Swell Activation can be Conferred on the Swell-insensitive mBest2

The structural domains necessary for swell-induced channel activation are unknown. Although dBest1 has a long poorly conserved C-terminus (Figure 4C), it is not necessary for swell activation. dBest1 remains swell-sensitive despite the removal of up to 338 of its C-terminal amino acid residues (Stop 383, Figure 4C; Figure 8A). Next we examined whether chimeras might reveal the domains underlying swell activation. dBest1's closest mammalian homolog, mBest2, is not activated by hypo-osmotic solutions (Figure 8B). Chimera d64m (the first 64 residues are dBest1; the remaining residues are identical to those of mBest2; Figure 4C) expression resulted in a constitutively active current that more than doubled with swelling (2.3 fold ±0.3 increase; Student's t-test, $p < 0.05$; Figure 8B–D). The d64m chimera maintained the relative permeability and slope conductance of mBest2 (Figure 8E & F; Table 1 & 2), suggesting that the channel's pore domain is downstream of residue 64. Two other groups have assessed mBest2 selectivity [44,45] and found greater permeability for SCN than we report here. Both groups used high intracellular calcium to activate I_{mBest2}; we report constitutive I_{mBest2} measured with high internal calcium buffering (i.e. <10 nM free calcium). Our HEK cell line was also screened for potentially contaminating I_{SCN} (data not shown) attributable to SLC1A family member expression [40]. The pharmacological profile of I_{d64m} noticeably diverged from both that of HEK $I_{Clswell}$ and I_{dBest1} (Figure 2). Furosemide blocked 75% of I_{d64m}, while DIDS and DCPIB both blocked I_{d64m} to near completion (Figure 2D). We conclude that the dBest1 N-terminal domain is required for swell activation of the mBest2 channel. The reverse chimera (m64d) was nonfunctional; exogenous currents were not observed with swelling or in the presence of high intracellular Ca^{2+} (data not shown). We cannot conclude with this data however, that the N-terminus is a "swelling" domain as it lacks any predictive motifs. We hypothesize that it works in concert with domains present both in dBest1 and mBest2 to facilitate swell activation. The strong correlation between S2R+ $I_{Clswell}$ and I_{dBest1}, combined with the unique selectivity and pharmacology of the d64m chimera, support the conclusion that the Bestrophin protein itself forms the Cl_{swell} channel rather than functioning as an auxiliary subunit.

Discussion

Our study validates the H148Q-YFP fluorophore as a reliable reporter of Cl_{swell} channel activity in genome-wide RNAi screening studies. H148Q-YFP has been employed very effectively in the identification of novel chloride channel activators, modulators, and blockers of CFTR and Ca^{2+}-activated Cl^- channels [18]. This is the first reported RNAi screen using an

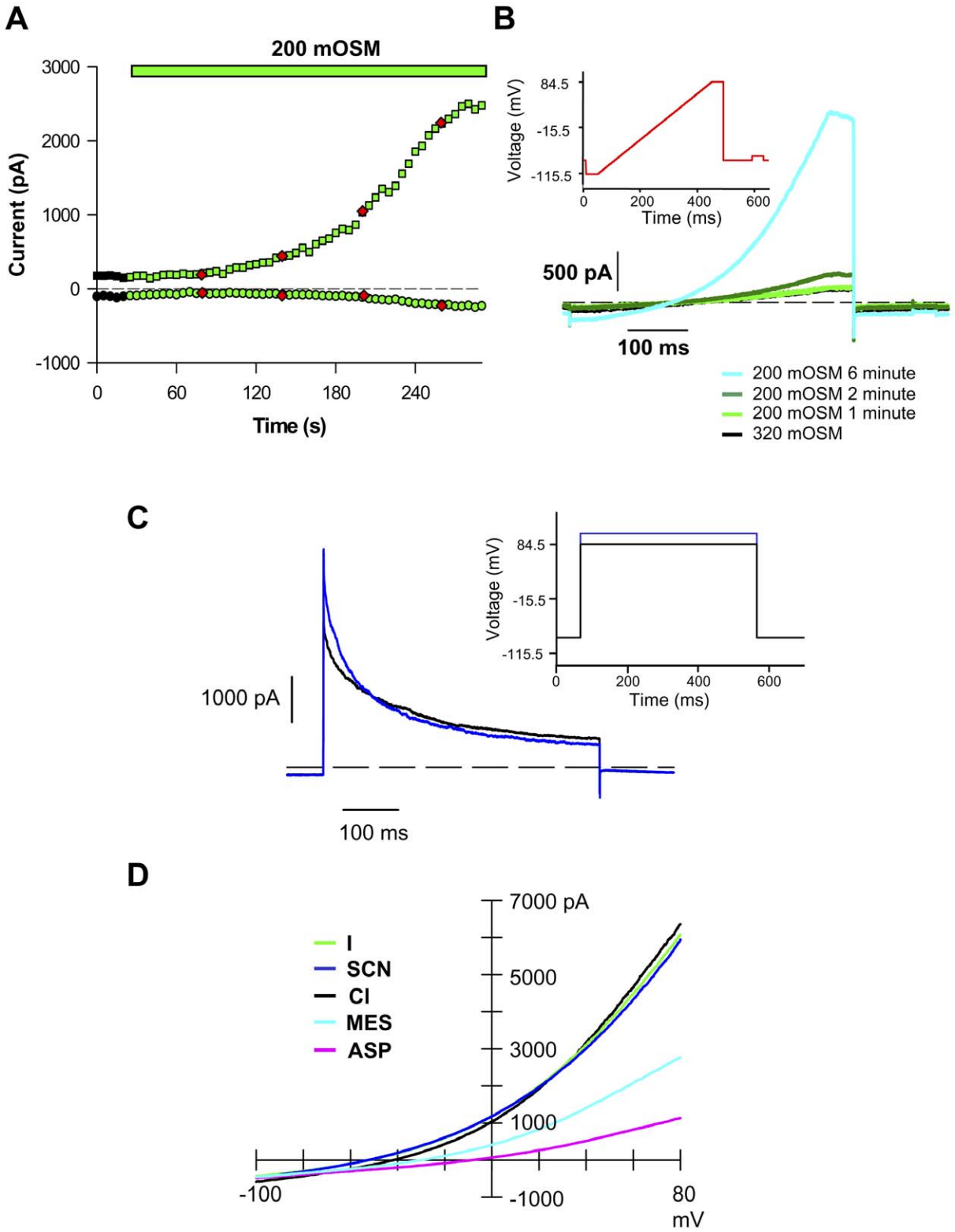

Figure 6. The endogenous HEK cell $I_{Clswell}$ has characteristic mammalian $I_{Clswell}$ properties. (**A**) HEK cell $I_{Clswell}$ develops slowly, reaching steady state after 5 min exposure to 200 mOSM solution. ◆ indicate min in 200 mOSM. (**B**) Ramp protocol (inset) assessment of the HEK $I_{Clswell}$. Little $I_{Clswell}$ has developed after 2 min in 200 mOSM solution. The steady state $I_{Clswell}$ is outwardly rectifying and inactivating at positive potentials. No tail currents are apparent. (**C**) Step protocol (inset) assessment of the HEK $I_{Clswell}$. Rapid inactivation is observed at positive potentials. No tail currents are apparent. (**D**) Relative permeability and slope conductance sequences for the endogenous HEK $I_{Clswell}$ are SCN = I > Cl >> MES > ASP vs SCN = I = Cl >> MES > ASP.

doi:10.1371/journal.pone.0046865.g006

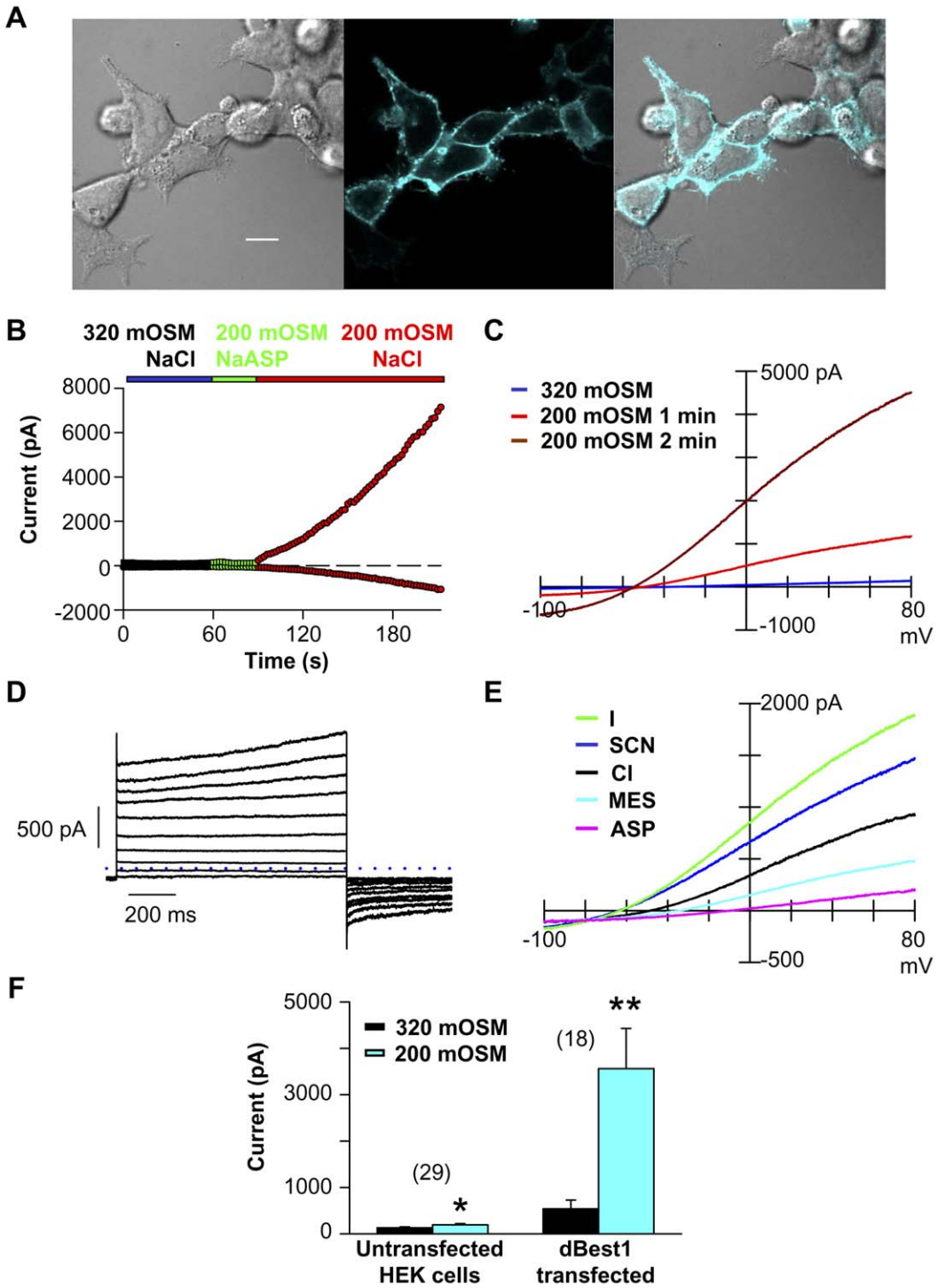

Figure 7. dBest1 overexpression in HEK cells produces a S2R+ cell-like $I_{Clswell}$. (**A**) dBest1-gfp targets to the membrane of HEK cells. Confocal images of dBest1-gfp overexpressed in HEK-293 cells. The DIC image is on the left, GFP in the middle, overlapped images on the right. Scale bar indicates 10 μm. (**B**) I_{dBest1} rapidly develops within the first 2 min of hypo-osmotic stimulation. (**C**) The developing I_{dBest1} has the same "S" shape rectification as the endogenous S2R+ cell $I_{Clswell}$. (**D**) Step protocol shows that I_{dBest1} shares time-dependent activation and tail current properties with S2R+ cell $I_{Clswell}$. (**E**) The constitutively active I_{dBest1} and S2R+ cell $I_{Clswell}$ selectivity sequences are very similar. (**F**) I_{dBest1} is clearly separable from the endogenous HEK cell $I_{Clswell}$. I_{dBest1} increases 15.8 fold ±4.5 (n = 18; ** paired Student's t-test, $p<0.005$) in the first 2 min of hypo-osmotic stimulation; the endogenous HEK cell $I_{Clswell}$ increases 2.1 fold ±0.4 (n = 29; * paired Student's t-test, $p<0.05$).
doi:10.1371/journal.pone.0046865.g007

anion-sensitive fluorescent protein to assign molecular identity to a chloride channel. Our screen supports the findings of the Hartzell lab [15]: dBest1 RNAi eliminates *Drosophila* $I_{Clswell}$.

We found that the RNAi effectiveness was essential for Cl_{swell} candidate identification. Two separate dBest1-targeting RNAi's were part of our initial screen: DRSC26457 and DRSC16909

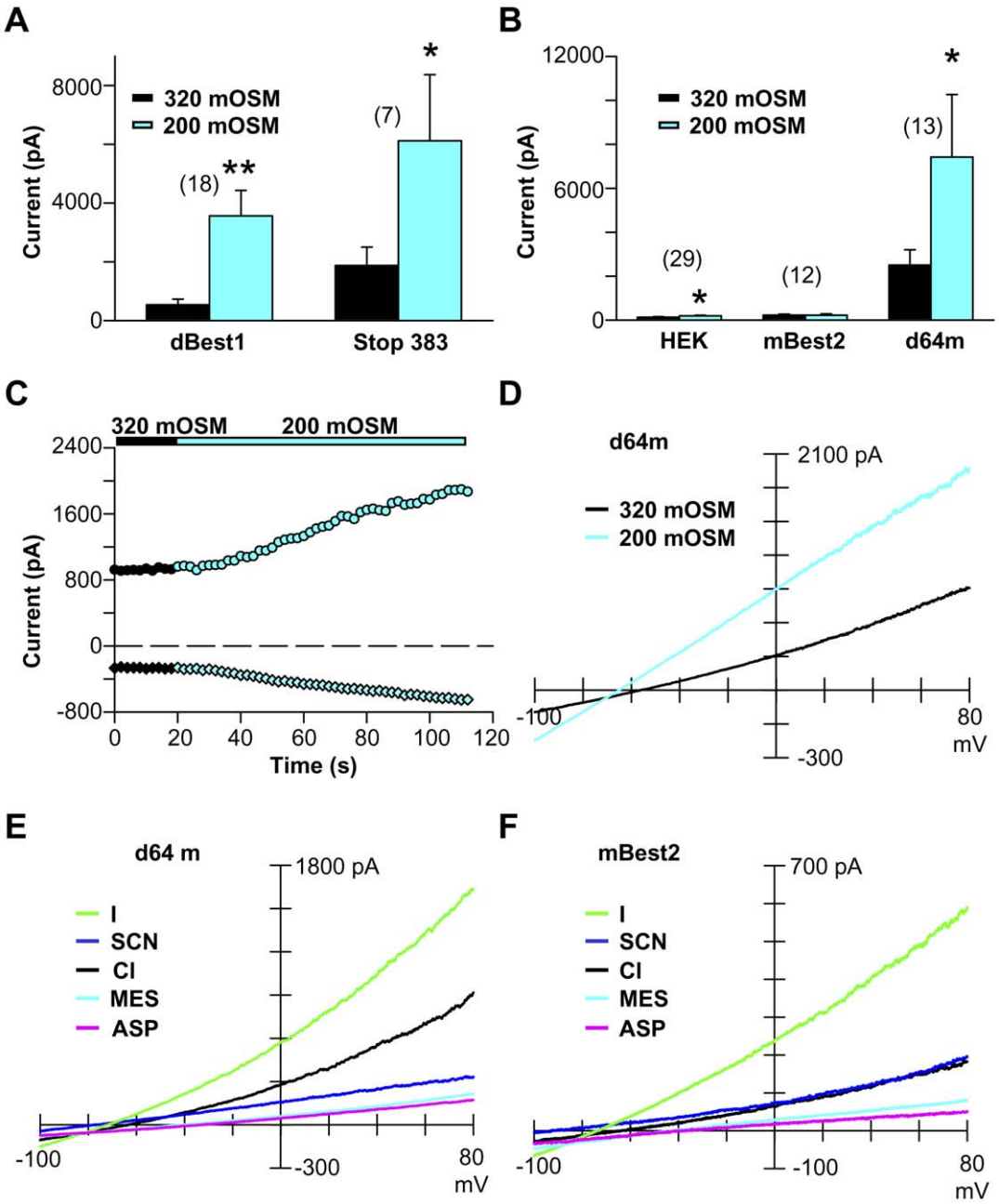

Figure 8. Chimeras between dBest1 and mBest2 confer swell activation on mBest2. (**A**) Truncation of dBest1 does not interfere with swell sensitivity. Constitutive currents are apparent with both dBest1 and Stop 383 overexpression in iso-osmotic solutions (320 mOSM). With swell, current increased dramatically for both constructs (Student's t-test, * $p<0.05$, ** $p<0.005$). (**B**) d94m current increases significantly within the first 2 min of swelling (* Student's t-test, $p<0.05$). (**C**) Time course for d64m swell activation. (**D**) Current-voltage relations for constitutive d64m, and following 2 min 200 mOSM solution. (**E**) Selectivity sequence for the constitutively active d64m current. (**F**) Selectivity sequence for the constitutively active mBest2 currents.
doi:10.1371/journal.pone.0046865.g008

(which corresponds to dB1S [15]), but only DRSC26457 was a hit. qPCR reported a 95% reduction in dBest1 mRNA with DRSC26457 treatment versus an 85% reduction with DRSC16909. Hartzell and colleagues found that S2 cell $I_{Clswell}$ was significantly reduced following treatment with 0.4 μg of DRSC16909 [15], while in our screen each assay well had a standardized 0.25 μg of RNAi. Using more RNAi may have effected greater target knockdown and resulted in the detection of DRSC16909 as a hit in our screen. This result emphasizes the importance of RNAi effectiveness in hit identification.

Exogenously expressed I_{dBest1} and endogenous S2R+ $I_{Clswell}$ share similar characteristics, including time-dependent activation, tail currents, relative permeability sequences, slope conductance sequences, and pharmacological profiles. The shared properties of *Drosophila* $I_{Clswell}$ and I_{dBest1} suggest that the same protein forms the channel responsible for both. Bestrophin is a known ion channel modulator, altering voltage-gated calcium channel activity [46]. If

dBest1 expression simply modulated or upregulated the endogenous HEK Cl_{swell} channel expression, we would have expected the resulting $I_{Clswell}$ to maintain the properties of HEK $I_{Clswell}$. Instead we observed that dBest1 introduced an exogenous *Drosophila*-like $I_{Clswell}$ whose development preceeded that of the endogenous HEK $I_{Clswell}$. I_{dBest1} matched the pharmacological profile of the S2R+ $I_{Clswell}$. Moreover, we found that the exogenous *Drosophila*-like $I_{Clswell}$ permeability and conductance sequence could be transformed into that of mBest2 with the d64m chimera. The pharmacological profile of I_{d64m} was again significantly different from the endogenous HEK $I_{Clswell}$. We conclude that dBest1 is the *Drosophila* Cl_{swell} channel.

Several Bestrophin mutations are associated with vitelliform macular dystrophy [36,37]. How these mutations are causally linked to the disease is not clear. Here we found that overexpression of the disease-linked W94C dBest1 mutant in S2R+ cells significantly suppressed the endogenous *Drosophila* $I_{Clswell}$. The W94C mutation occurs in the putative pore of dBest1 and thus may disrupt Cl_{swell} conductance. However, the fluorescently tagged W94C dBest1 protein appears to localize to intracellular compartments, consistent with mislocalization. Milenkovic *et al*, have recently proposed that disease-associated Bestrophin mutations cause defects in intracellular trafficking [38]. Both scenarios may explain the dominant negative effect of dBest1 W94C on *Drosophila* $I_{Clswell}$: non-functional, pore-disrupting, mutant Bestrophin proteins complexing with wild-type dBest1 may be largely retained within the endoplasmic reticulum. The end result would be the elimination of endogenous *Drosophila* $I_{Clswell}$. Our experiments support the hypothesis that mutant Bestrophin W93C expression could significantly disrupt chloride flux and homeostasis in the human macula, contributing to the disease state.

The distinction of Bestrophin function in *Drosophila* versus mammalian cells is most clearly illustrated by Hartzell and colleagues [16]. $I_{Clswell}$ measured in peritoneal mast cells isolated from *mBest1*$_{-/-}$, *mBest2*$_{-/-}$, and *mBest*1/2 double knockout mice was identical to *wild-type* $I_{Clswell}$. hBest1 and mBest2 are swell sensitive in that their currents are inhibited by hyperosmotic solutions. However, their activity does not increase with swell [12]. We confirm here that mBest2 activation does not increase when cells swell. Our d64m chimera contained only a small portion of dBest1, yet it responded to cellular swelling. The crucial N-terminal region contains no distinct association domains or predictive structures that might explain its coupling to changes in cell stretch, tension, or osmolality. We speculate that the N-terminus contributes to a required tertiary structure that enables swell signaling events to activate the dBest1 channel.

Our genome-wide RNAi screen of S2R+ cells and follow-up study firmly establishes that the dBest1 protein forms the *Drosophila* Cl_{swell} channel. It further validates a live cell genetically engineered fluorescent screening platform to identify other mammalian chloride channels.

Materials and Methods

Generation of the S2R+ YFP- H148Q Stable Cell Line

The stable S2R+ cell line expressing a halide-sensitive YFP (H148Q-YFP; kindly provided by Dr. Alan Verkman, UCSF) was generated with a selection vector (pCoBlast). H148Q-YFP was subcloned into the pAc5.1/V5-HisA vector (Invitrogen, CA). The S2R+ cells were transfected by electroporation (Amaxa cell line nucleofector kit V; Lonza). Cells were placed under selective pressure with 25 μg/ml blasticidin for 2 weeks. Two rounds of fluorescence-activated cell sorting (FACS; DFCI Flow Cytometry Core Facility) normalized YFP fluorescence intensities. These S2R+ cells exhibited a robust $I_{Clswell}$ as described in Figure 1. S2R+ cells were maintained in Schneider's *Drosophila* medium (Invitrogen), with 10% heat inactivated fetal bovine serum (Invitrogen), and 1% penicillin/streptomycin (Sigma-Aldrich). For the primary screen, cells were spun down and resuspended in serum-free medium at a density of 9×10^4 cells/ml. 10 μl of the cell suspension was added to each of the 384 wells using the Matrix Wellmate 8-channel microplate dispenser (ThermoScientific; DRSC). Cells were incubated for 30 min, then 30 μl of serum containing medium were added to each well. Cells were cultured for 5 d before the swell assay was performed (5 d RNAi treatment is necessary to sufficiently knock down proteins with slow turnover rates). For the secondary screen, cells were plated at a density of 40% in a 6 well dish. Once cells were adherent, the medium was replaced with 1 ml of serum-free medium containing 0.015 μg/μl dsRNA. Cells were incubated for 30 min at room temperature followed by addition of 3 ml of serum-containing medium to each well. Transfections were performed in duplicate; 1 well was used for functional studies and the other for qPCR analysis of knockdown at day 5.

Screening Solutions

Iso-osmotic (320 milliOsm/kg; mOSM) solutions contained in mM: 105 NaCl or NaI, 2 $CaCl_2$, 1 $MgCl_2$, 5 KCl, 10 HEPES, 10 Glucose, 90 Mannitol (pH 7.4 NaOH). For hypo-osmotic (240 mOSM) solutions, mannitol was omitted. 1 mM furosemide (Sigma-Aldrich) blocked 100% of the S2R+ $I_{Clswell}$ and prevented significant H148Q-YFP suppression. Furosemide is a specific blocker of Na-K-2Cl co-transporters (SLC12A2) at concentrations in the μM range.

The Primary Screen

Our genome-wide screen was conducted at the Harvard/HHMI *Drosophila* RNAi Screening Center using the DRSC 2.0 Genomewide RNAi Library. DRSC 2.0 is a collection of dsRNAs for genome-wide RNAi knockdown covering ~ 13,900 genes encoding proteins and non-coding RNAs while minimizing off-target effects due to sequence similarity to other genes. Each gene is targeted by 1.3 dsRNA/gene. The screen consisted of 66 384-well assay plates in duplicate. Each well of the 384-well plate contained 5 μl of 0.05 μg/μl dsRNA in water (0.25 μg dsRNA/well). Each plate contained control RNAi specific for *Thread* (*Drosophila* inhibitor of apoptosis protein), *Rho* (a small GTPase activator of the EGFR signaling pathway), and *GFP*. On day 5 of RNAi treatment, the cellular fluorescence of the H148Q-YFP probe was measured under several treatment conditions using the Analyst GT plate reader (Molecular Devices; DRSC). The probe was excited at 485 nm and emissions collected at 530 nm. Before fluorescence measurements were taken, the media was aspirated (384-well aspirator; VP Scientific) and the cells were equilibrated in 80 μl of 320 mOSM NaCl solution. After 10 min this solution was removed by aspiration and cells incubated in 240 mOSM NaCl for 5 min. Fluorescence was then measured, the NaCl solution removed and cells were incubated in 240 mOSM NaI for 5 min. Fluorescence was again measured; the change in fluorescence was determined by dividing the fluorescence in 240 mOSM NaI by that in 240 mOSM NaCl. Wells with fluorescence or ratio changes (240 mOSM I^- fluorescence/240 mOSM Cl^- fluorescence) greater than 1.5 times the standard deviation (1.5×S.D.) of the plate mean were initially considered as hits (candidates of Cl_{swell} channel or regulators of its activation pathway). False positives could potentially result if the RNAi treatment caused a

high internal pH as H148Q-YFP has a pKa of 6.7. Cell death was detected in control wells indicating effective RNAi treatment.

Generation of dsRNA

cDNA templates were generated by PCR amplification of genomic DNA using primers designed by the DRSC (SnapDragon tool). These primers had the T7 promoter sequence (TAATACGACTCACTATAGGG) added to the 5' end of both primers. The templates generally corresponded to exons but occasionally sequences with two or more exons interrupted by introns were used. The PCR fragments were ~150–600 base pairs in length, and any complete 19-mer homology to other genes that could lead to non-specific dsRNA are reported. Individual RNAi sequences used here are found in the DRSC website (www.flyrnai.org). dsRNAs against *Drosophila* were synthesized with the MEGAscript in vitro transcription kit (Ambion). RNA was purified with the RNeasyPlus mini kit (Qiagen) and stored at −80°C.

qPCR Analysis of RNAi Efficiency

After 5 d RNAi treatment, RNA was prepared from the S2R+ cells using the RNeasy Plus mini kit (Qiagen). 2.5 μg RNA was used for each first-strand cDNA synthesis reaction (SuperScript Vilo cDNA Synthesis kit, Invitrogen). Primers for qPCR were designed on the NCBI/PrimerBlast site (http://www.ncbi.nlm. nih.gov/tools/primer-blast/) with the following restrictions: PCR product size was between 70 and 300 bp, primer melting temperatures were between 57 and 63°C, primers spanned an exon-exon junction, and primers were specific to the intended PCR template as determined by BLAST analysis of the *Drosophila melanogaster* Refseq mRNA database. Primer sets were only used if the melting curve had a single peak. The RT^2 Real-Time SYBR Green/Rox PCR master mix (SABiosciences) was used for qPCR. qPCR reactions were set up in quadruplicate to minimize pipetting errors, and run on the Mastercycler ep Realplex real-time PCR system (Eppendorf). Average cycle numbers for each primer set were normalized to either dTaf8 or dAct79b average cycle numbers.

Secondary Screening of Candidates

Comprehensive bioinformatics analysis of the hit list was performed to identify potential candidates for Cl_{swell}. Hits were limited to those with human homologs and at least a single transmembrane domain. Potential regulators of the Cl_{swell} activation pathway were left for future consideration. The effects of RNAi on fluorescence changes were confirmed by plate reader or imaging experiments. The specificity and effectiveness of the RNAi was assessed by qPCR. S2R+ cells treated with RNAi were patch clamped and $I_{Clswell}$ was directly measured. Candidates were cloned and expressed in HEK293 or CHO-K1 cells. $I_{Clswell}$ was measured by whole-cell patch clamp recording.

Electrophysiology

Whole-cell patch clamp recordings were made at room temperature. Recordings were obtained using an Axopatch 200B amplifier, Digidata 1322A analog-to-digital converter, and pClamp 8.01 software (Molecular Devices, Union City, CA). Data were low-pass filtered at 2 kHz and digitized at 5 kHz. Fire-polished thin or thick wall borosilicate glass pipettes of 3–4 MΩ resistances were used for recordings; access resistance was compensated to >80%. Cells were held at −70 mV to clearly eliminate cells with leaky seals and voltage ramps (400 ms in duration) from −100 to +100 mV were applied every 2–5 s. Liquid junction potentials were corrected during analysis, and ramp data were plotted between −100 and +80 mV.

Recording Solutions

Internal pipette solution contained (in mM): 160 CsASP, 10 Cs4BAPTA, 4 MgATP, 2 $MgCl_2$, 8 NaCl, and 10 HEPES (pH 7.4 with CsOH). 10 mM BAPTA was used to prevent activation of channels by calcium and to reduce the endogenous HEK cell $I_{Clswell}$, which is optimally activated with 100 nM Ca_i [47]. 240 mOSM solution composition is detailed in 'Screening solutions'. 200 mOSM solutions contained in mM: 82.5 NaCl, NaI, NaSCN, NaMES, or NaASP, 2 $CaCl_2$, 1 $MgCl_2$, 5 KCl, 10 HEPES, and 10 Glucose (pH 7.4 with NaOH). 90 mM mannitol was added to bring osmolality to 320 mOSM. The relative permeabilities were estimated from the Goldman-Hodgkin-Katz equation. For our calculations, the $[Cl]_i$ was set to 0 mM. Cells were held at -70 mV during all recordings, rapidly depleting Cl_i. Cation permeability was essentially nil, as replacement of 200 mOSM NaCl solution with 200 mOSM NMDG-Cl solution did not change the reversal potential (E_{rev}; data not shown). Slope conductances were calculated for each anionic substitution between the E_{rev} and +80 mV. For the S2R+ and HEK cells E_{rev} and $I_{+80\ mV}$ were measured in 200 mOSM solutions. For exogenously expressed dBest1, mBest2, and d64m E_{rev} and $I_{+80\ mV}$ were measured in 320 mOSM solutions to prevent contamination with the endogenous HEK cell $I_{Clswell}$. The HEK cell line chosen for over-expression studies had no constitutive I_{Cl} ($I_{320\ mOSM}$ did not change when switching between Cl and ASP), the endogenous $I_{Clswell}$ developed very slowly, and the cells did not have an endogenous I_{SCN} (attributable to SLC1A family member expression [40].

Pharmacology

Stock solutions of DIDS (0.1 M in DMSO; Sigma), DCPIB (50 mM in EtOH; Tocris), and furosemide (1M in DMSO; Sigma) were prepared and diluted in 320 mOSM or 200 mOSM NaCl solution to their final concentrations.

Molecular Biology

dBest1 was a kind gift from Dr. Criss Hartzell (Emory University). All other constructs were either ordered from Open Biosystems or cloned from a *Drosophila* cDNA library or Human Brain (whole Marathon ready cDNA library; BD Biosciences). Candidate cDNAs were subcloned into pEGFP-N3 (C-terminal tag; BD Biosciences) and an engineered Red pTracer vector (untagged). We found that an N-terminal EGFP tag rendered dBest1 nonfunctional (data not shown). Using site-directed mutagenesis we introduced the W94C mutation into *dBest1* pEGFP-N3 (GeneArt site-directed mutagenesis, Invitrogen, CA). *dBest1* W94C-gfp was then subcloned into the pAc5.1 V5-HisA vector (Invitrogen, CA).

Supporting Information

Figure S1 The late activating component of S2R+ $I_{Clswell}$ remains despite overexpression of dBest1 W94C-gfp. (**A**) The late activating component of S2R+ $I_{Clswell}$ is isolated after dominant negative elimination of I_{dBest1}. Inset: Step protocol. (**B**) The late activating component of S2R+ $I_{Clswell}$ is sharply rectifying (ramp protocol; inset). Red trace is 320 mOSM solution, blue trace is 80 s after the 200 mOSM solution change. The late activating $I_{Clswell}$ develops after 36 s in 200 mOSM solution.
(TIF)

Table S1 Secondary screening identifies Best1 as the *Drosophila* Cl_{swell} channel. Candidates with transmembrane domains and human homologs were further studied to determine if they formed the Cl_{swell} channel. ✓ indicates a positive secondary screening result; X indicates a negative result. ☆ indicates that several qPCR primer sets consistently had more than 1 melting

point peak suggesting nonspecific primer binding. The effectiveness of RNAi knockdown, therefore, could not be determined by qPCR. ?? indicates that two cells overexpressing SLC1A2 had substantial I_{SCN-} currents but small $I_{Clswell}$. Thus, SLC1A2 overexpression may upregulate endogenous HEK cell $I_{Clswell}$ in the majority of the population but does not form the channel itself. HeLa cells treated with SLC1A3 siRNA (which reduced SLC1A2 and SLC1A3 mRNA by 90% and 92% respectively) had unaltered $I_{Clswell}$ (data not shown).
(TIF)

Acknowledgments

We thank the *Drosophila* RNAi Screening Center at Harvard Medical School (NIH/NIGMS 2R01GM067761) for providing RNAi libraries, laboratory space, bioinformatics tools and other support for the screen.

Author Contributions

Conceived and designed the experiments: SCS. Performed the experiments: SCS. Analyzed the data: SCS. Contributed reagents/materials/analysis tools: SCS DEC. Wrote the paper: SCS DEC.

References

1. Nilius B, Eggermont J, Voets T, Buyse G, Manolopoulos V, et al. (1997) Properties of volume-regulated anion channels in mammalian cells. Prog Biophys Mol Biol 68: 69–119.
2. Baumgarten CM, Clemo HF (2003) Swelling-activated chloride channels in cardiac physiology and pathophysiology. Prog Biophys Mol Biol 82: 25–42.
3. d'Anglemont de Tassigny A, Souktani R, Ghaleb B, Henry P, Berdeaux A (2003) Structure and pharmacology of swelling-sensitive chloride channels, I(Cl,swell). Fundam Clin Pharmacol 17: 539–553.
4. Grunder S, Thiemann A, Pusch M, Jentsch TJ (1992) Regions involved in the opening of CIC-2 chloride channel by voltage and cell volume. Nature 360: 759–762.
5. Duan D, Winter C, Cowley S, Hume JR, Horowitz B (1997) Molecular identification of a volume-regulated chloride channel. Nature 390: 417–421.
6. Gill DR, Hyde SC, Higgins CF, Valverde MA, Mintenig GM, et al. (1992) Separation of drug transport and chloride channel functions of the human multidrug resistance P-glycoprotein. Cell 71: 23–32.
7. Valverde MA, Diaz M, Sepulveda FV, Gill DR, Hyde SC, et al. (1992) Volume-regulated chloride channels associated with the human multidrug-resistance P-glycoprotein. Nature 355: 830–833.
8. Paulmichl M, Li Y, Wickman K, Ackerman M, Peralta E, et al. (1992) New mammalian chloride channel identified by expression cloning. Nature 356: 238–241.
9. Krapivinsky GB, Ackerman MJ, Gordon EA, Krapivinsky LD, Clapham DE (1994) Molecular characterization of a swelling-induced chloride conductance regulatory protein, pICln. Cell 76: 439–448.
10. Landry D, Sullivan S, Nicolaides M, Redhead C, Edelman A, et al. (1993) Molecular cloning and characterization of p64, a chloride channel protein from kidney microsomes. J Biol Chem 268: 14948–14955.
11. Moorman JR, Palmer CJ, John JE, 3rd, Durieux ME, Jones LR (1992) Phospholemman expression induces a hyperpolarization-activated chloride current in Xenopus oocytes. J Biol Chem 267: 14551–14554.
12. Fischmeister R, Hartzell HC (2005) Volume sensitivity of the bestrophin family of chloride channels. J Physiol 562: 477–491.
13. Almaca J, Tian Y, Aldehni F, Ousingsawat J, Kongsuphol P, et al. (2009) TMEM16 proteins produce volume-regulated chloride currents that are reduced in mice lacking TMEM16A. J Biol Chem 284: 28571–28578.
14. Martins JR, Faria D, Kongsuphol P, Reisch B, Schreiber R, et al. (2012) Anoctamin 6 is an essential component of the outwardly rectifying chloride channel. Proc Natl Acad Sci U S A 108: 18168–18172.
15. Chien LT, Hartzell HC (2007) Drosophila bestrophin-1 chloride current is dually regulated by calcium and cell volume. J Gen Physiol 130: 513–524.
16. Chien LT, Hartzell HC (2008) Rescue of volume-regulated anion current by bestrophin mutants with altered charge selectivity. J Gen Physiol 132: 537–546.
17. Richards MW, Butcher AJ, Dolphin AC (2004) Ca2+ channel beta-subunits: structural insights AID our understanding. Trends Pharmacol Sci 25: 626–632.
18. Verkman AS, Galietta LJ (2009) Chloride channels as drug targets. Nat Rev Drug Discov 8: 153–171.
19. Wachter RM, Yarbrough D, Kallio K, Remington SJ (2000) Crystallographic and energetic analysis of binding of selected anions to the yellow variants of green fluorescent protein. J Mol Biol 301: 157–171.
20. Worby CA, Dixon JE (2004) RNA interference in cultured Drosophila cells. Curr Protoc Mol Biol Chapter 26: Unit 26 25.
21. Schneider I (1972) Cell lines derived from late embryonic stages of Drosophila melanogaster. J Embryol Exp Morphol 27: 353–365.
22. Kennerdell JR, Carthew RW (1998) Use of dsRNA-mediated genetic interference to demonstrate that frizzled and frizzled 2 act in the wingless pathway. Cell 95: 1017–1026.
23. Misquitta L, Paterson BM (1999) Targeted disruption of gene function in Drosophila by RNA interference (RNA-i): a role for nautilus in embryonic somatic muscle formation. Proc Natl Acad Sci U S A 96: 1451–1456.
24. Yanagawa S, Lee JS, Ishimoto A (1998) Identification and characterization of a novel line of Drosophila Schneider S2 cells that respond to wingless signaling. J Biol Chem 273: 32353–32359.
25. Jentsch TJ, Stein V, Weinreich F, Zdebik AA (2002) Molecular structure and physiological function of chloride channels. Physiol Rev 82: 503–568.
26. Decher N, Lang HJ, Nilius B, Bruggemann A, Busch AE, et al. (2001) DCPIB is a novel selective blocker of I(Cl,swell) and prevents swelling-induced shortening of guinea-pig atrial action potential duration. Br J Pharmacol 134: 1467–1479.
27. Jayaraman S, Haggie P, Wachter RM, Remington SJ, Verkman AS (2000) Mechanism and cellular applications of a green fluorescent protein-based halide sensor. J Biol Chem 275: 6047–6050.
28. Galietta LJ, Haggie PM, Verkman AS (2001) Green fluorescent protein-based halide indicators with improved chloride and iodide affinities. FEBS Lett 499: 220–224.
29. Kuner T, Augustine GJ (2000) A genetically encoded ratiometric indicator for chloride: capturing chloride transients in cultured hippocampal neurons. Neuron 27: 447–459.
30. Galietta LV, Jayaraman S, Verkman AS (2001) Cell-based assay for high-throughput quantitative screening of CFTR chloride transport agonists. Am J Physiol Cell Physiol 281: C1734–1742.
31. Markova O, Mukhtarov M, Real E, Jacob Y, Bregestovski P (2008) Genetically encoded chloride indicator with improved sensitivity. J Neurosci Methods 170: 67–76.
32. Tsunenari T, Sun H, Williams J, Cahill H, Smallwood P, et al. (2003) Structure-function analysis of the bestrophin family of anion channels. J Biol Chem 278: 41114–41125.
33. Hartzell C, Putzier I, Arreola J (2005) Calcium-activated chloride channels. Annu Rev Physiol 67: 719–758.
34. Hartzell HC, Qu Z, Yu K, Xiao Q, Chien LT (2008) Molecular physiology of bestrophins: multifunctional membrane proteins linked to best disease and other retinopathies. Physiol Rev 88: 639–672.
35. Marmorstein AD, Cross HE, Peachey NS (2009) Functional roles of bestrophins in ocular epithelia. Prog Retin Eye Res 28: 206–226.
36. Sun H, Tsunenari T, Yau KW, Nathans J (2002) The vitelliform macular dystrophy protein defines a new family of chloride channels. Proc Natl Acad Sci U S A 99: 4008–4013.
37. Qu Z, Wei RW, Mann W, Hartzell HC (2003) Two bestrophins cloned from Xenopus laevis oocytes express Ca(2+)-activated Cl(-) currents. J Biol Chem 278: 49563–49572.
38. Milenkovic VM, Rohrl E, Weber BH, Strauss O (2012) Disease-associated missense mutations in bestrophin-1 affect cellular trafficking and anion conductance. J Cell Sci 124: 2988–2996.
39. Xiao Q, Prussia A, Yu K, Cui YY, Hartzell HC (2008) Regulation of bestrophin Cl channels by calcium: role of the C terminus. J Gen Physiol 132: 681–692.
40. Melzer N, Biela A, Fahlke C (2003) Glutamate modifies ion conduction and voltage-dependent gating of excitatory amino acid transporter-associated anion channels. J Biol Chem 278: 50112–50119.
41. Gosling M, Smith JW, Poyner DR (1995) Characterization of a volume-sensitive chloride current in rat osteoblast-like (ROS 17/2.8) cells. J Physiol 485 (Pt 3): 671–682.
42. Eggermont J (2004) Calcium-activated chloride channels: (un)known, (un)loved? Proc Am Thorac Soc 1: 22–27.
43. Kunzelmann K, Milenkovic VM, Spitzner M, Soria RB, Schreiber R (2007) Calcium-dependent chloride conductance in epithelia: is there a contribution by Bestrophin? Pflugers Arch 454: 879–889.
44. Qu Z, Fischmeister R, Hartzell C (2004) Mouse bestrophin-2 is a bona fide Cl(-) channel: identification of a residue important in anion binding and conduction. J Gen Physiol 123: 327–340.
45. O'Driscoll KE, Leblanc N, Hatton WJ, Britton FC (2009) Functional properties of murine bestrophin 1 channel. Biochem Biophys Res Commun 384: 476–481.
46. Yu K, Xiao Q, Cui G, Lee A, Hartzell HC (2008) The best disease-linked Cl-channel hBest1 regulates Ca V 1 (L-type) Ca2+ channels via src-homology-binding domains. J Neurosci 28: 5660–5670.
47. Szucs G, Heinke S, Droogmans G, Nilius B (1996) Activation of the volume-sensitive chloride current in vascular endothelial cells requires a permissive intracellular Ca2+ concentration. Pflugers Arch 431: 467–469.